

# Robotic Relocalization Algorithm Assisted by Industrial Internet of Things and Artificial Intelligence

Bi Zeng<sup>1</sup>, Shuang Yang<sup>1</sup>, Xiuwen Yin<sup>2</sup>

<sup>1</sup> School of Computers, Guangdong University of Technology, China

<sup>2</sup> School of Automation, Guangdong University of Technology, China  
zb9215@gdut.edu.cn, ys950731@163.com, yxw@gdut.edu.cn

## Abstract

The Industrial Internet of Things (IIoT) scheme has the ability to integrate the computing center and the terminal actuator. It is usually the basis for the effective work of some IIoT systems that the terminal actuator can provide highly-precise location information. Under the assistance of the IIoT, we target at proposing a robot relocalization algorithm with high accuracy and stability in this paper. The relocalization method employing both semantic laser and landmark information is first designed, in which laser sensors are used to obtain quantitative information while semantic information is obtained using visual sensors. A pose derivation model based on the acquired landmark information is presented to correct the position of the actuator. In addition, the reinforcement learning is employed to dynamically select the optimal motion information during the relocalization process, based on which the positioning results are continuously optimized. The experimental results show that the proposed method has high accuracy and stability.

**Keywords:** Relocalization, IIoT, Mobile robot, YOLOv3

## 1 Introduction

In recent years, the rapid development of wireless communication technologies has made it possible to integrate the computing center and the terminal actuator through Industrial Internet of Things (IIoT), which has great potential to optimize the factory production process with better efficiency, production plan and quality control [1]. However, as some issues, such as control accuracy, scalability and security, are still not addressed, the potential of IIoT is still not fully realized at present, which makes the IIoT a very attractive research area for researchers for years [2-8]. In [3], a quality of experience (QoE)-aware model for dynamic resource allocation is presented for tactile applications in IIoT, in which fog computing is adopted to provide computational and storage resources in close proximity to users. The authors in [5] concern the threat

of the targeted ransomware to the IIoT edge gateway, in which the anatomy of ransomware for edge gateways, the likelihood of the attack and motivations of the threat are researched. In [8], an adaptive transmission architecture and approach with software defined network (SDN) and edge computing for IIoT is proposed, which has potential to significantly improve the performance of IIoT.

With the rapid development of computing and communication techniques, such as edge computing and 5G, the Internet of Things (IoT), such as Internet of vehicle and IIoT, can provide strong network services for the terminal actors [9]. On the other hand, the location information of the terminal actor is usually the basis for the effective work of some IoT. For example, the indoor mobile robot can perform relevant operations automatically according to the location information or the command of the control center. To the IIoT-based control system which highly depends on the position information of the terminal actuator, improving the accuracy of the localization operation through relocalization algorithm is of great value to the improvement of the control accuracy of the system.

Up to now, a variety of positioning algorithms, such as the Monte Carlo localization algorithm based on the principle of particle filtering, have been employed in practical robot simultaneous localization and mapping (SLAM) applications [10-13]. In [11-12], the scanning matching process in SLAM has been improved, which not only improves the performance of the observation matching and pose estimation but also the dependence of the algorithm on the environmental features. However, its information dependence on the odometer (relevant method of recording speed, displacement, etc.) is too high, and the observation sensitivity is not enough, which make the performance of it is not high in the dynamic scene with few features. In recent years, the visual SLAM algorithms based on depth image information is developing rapidly, as shown in [14-20]. These algorithms use the landmark in the environment as a reference object to correct the robot pose, which can artificially use a small number of landmarks in the

\*Corresponding Author: Xiuwen Yin; E-mail: yxw@gdut.edu.cn

area, and enrich the feature information of the area. In addition, graph optimization is also employed to improve the accuracy of matching comparison to optimize positioning accuracy. However, in these algorithms, the more reliable observation information is commonly required to obtain better position estimation accuracy.

In addition, a phenomenon of positional drift will appear in positioning process in the long-term motion. To correct the pose drift and retrieve the initial positioning, the closed-loop detection method, which can be used to find the best match with the current key frame in the past key frames to optimize the trajectory of the robot, is adopted in [16-18]. Though these algorithms can obtain high positioning accuracy, the pose correction result is unstable because the visual sensor used is susceptible to many practical factors such as light and observation orientation. Therefore, in the environment that robots navigate in indoor environments, the SLAM technology based on multi-sensor data fusion is currently a hot research direction [21-23]. In [24-27], the robot corrects its own motion trajectory by adopting reinforcement learning to optimize the positioning results. However, most of these methods are designed to only optimize the planned path by learning the trajectory offset during the robot motion process.

Based on these research foundations, an adaptive localization algorithm (ALA) based on the semantic laser data and landmark objects in the SLAM process is proposed in this paper, which combines the semantic laser information with laser perception and visual recognition. To improve the positioning efficiency of the robot in the SLAM process, the landmark objects is abstracted in the map environment and be used to build a landmark database. The reinforcement learning is adopted to correct the robot error location and dynamically select the odometer data source for each localization process. The solution is not easily affected by environmental factors, which can be adapted in indoor dynamic scenes with high positioning robustness.

In addition, most of the aforementioned algorithms focus on optimizing the robot relocalization under the environment without efficient Internet connection. However, with the popularization and development of wireless sensor and actuator network (WSAN), machines and equipment in the factory environment supporting IIoT can usually get efficient Internet connection. For example, a typical IIoT network structure is shown in Figure 1, in which the edge computing server can provide efficient Internet access and powerful data computing for the terminal actuator with very short data transmission delay.

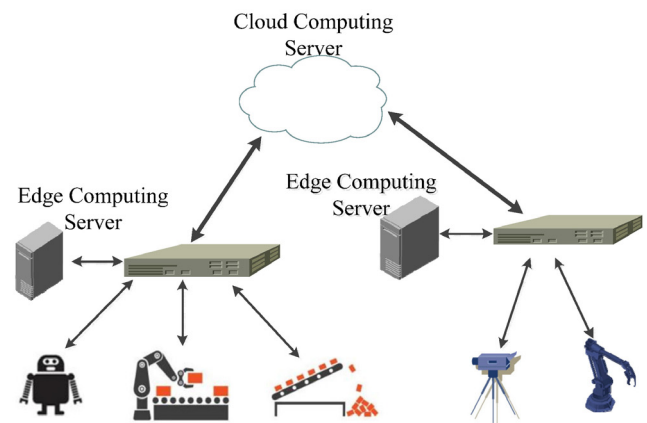


Figure 1. A typical IIoT network structure

In this paper, we target at proposing a robot relocalization algorithm with high accuracy and stability for the IIoT environment. Based on the assistance of the IIoT, a relocalization method employing both semantic laser and landmark information is designed, in which laser sensors is used to obtain quantitative information while semantic information is obtained using visual sensors. A pose derivation model based on the acquired landmark information is presented to correct the position of the actuator. In addition, the reinforcement learning is employed to dynamically select the optimal motion information during the relocalization process.

The rest of the paper is organized as follows: Section II shows the problem formulation. The proposed scheme is shown in Section III. In Section IV, the evaluation results are presented. A conclusion is drawn in Section V.

## 2 Problem Formulation

In the daily driving process, even if there are global positioning tools, humans still easily lose the way when passing through some complicated and remote road sections. It is often necessary to use roadside signs or landmark buildings to confirm their location. The same is true for robots. Even if they have the ability to localize in the map environment, they are vulnerable to environmental factors. When entering dynamic scenes with few features, the robot still easy lose its position and cannot perform independent reinforcement learning.

## 3 The Proposed Scheme

Based on the assistance of IIoT, a relocalization algorithm using both visual sensors and laser sensor is proposed in this paper, in which semantic laser and landmark information is employed to obtain quantitative information and semantic information, and enhanced learning technique is adopted to improve the positioning efficiency. The approach can avoid the misidentification

and mismatching caused by too similar laser data, and errors caused by the factors that can affect the visual detection, which means the algorithm is suitable for the indoor dynamic environment. The overall structure of the algorithm is shown in Figure 2.

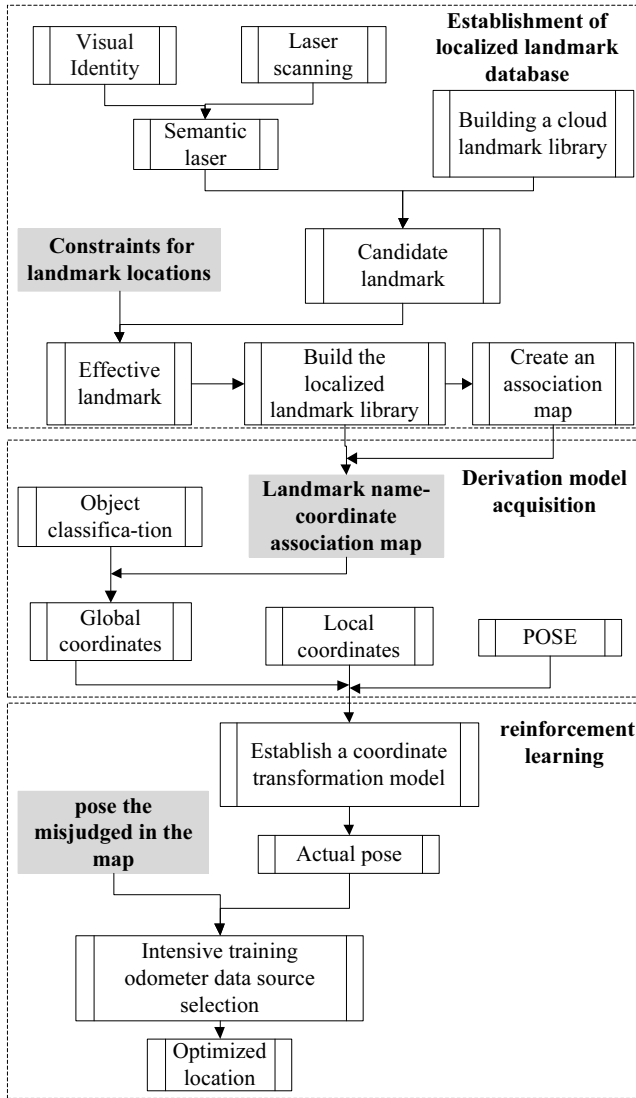


**Figure 2.** The overall architecture of the relocalization algorithm

### 3.1 Landmark Database Establishment

#### 3.1.1 The Cloud Landmark Database

In the proposed algorithm, a cloud landmark library, which is equivalent to the licenser, should be first build. With the assistance of efficient IIoT network, each robot can find the candidate landmarks in the current environment by searching the data content in the cloud landmark database. The landmark library in the cloud database is called candidate landmark library. In the process of constructing the cloud landmark library, the most critical part is the setting of the screening conditions that are used to judge whether the object has the qualification to become a landmark. The principles for setting the conditions are as follows:

- (1) The image characteristics of the object should be conspicuous, such as bright colors, rich styles.
- (2) The shape of the object is as flat as possible. In addition, if the shape or location of the object changes easily, the object should be excluded.

#### 3.1.2 The Localized Landmark Library

In the process of drawing, a number of localized landmark libraries need to be established based on the cloud landmark library, as the candidate landmarks acquired from the cloud landmark library are difficult to meet some actual requirements, such as response delay and search efficiency. The relative locational relationship between candidate landmarks should be used to judge and select the landmark objects available according to the local environment.

By exploring the real-time data transmission capability of the IIoT system, the local edge sever, which can transmit data to robots with a high data rate, is used to build the local landmark library. The diagrammatic sketch for the landmark database system is shown in Figure 3. Several localized landmark sub-databases are build at the local edge sever to obtain the effective landmarks according to the actual environment. In this way, we can compress the size of the local landmark database and improve the efficiency of the landmark retrieval.

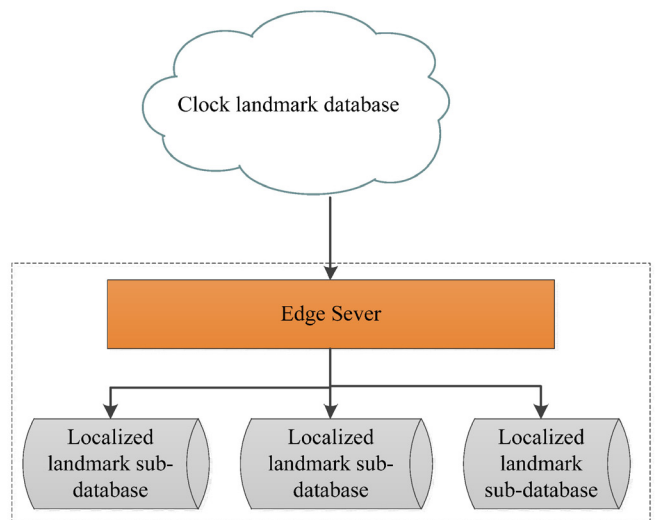


**Figure 3.** The landmark database system

The constraints for building the relative locational relationships are set to:

- (1) The location of the landmarks should be selected in places that are not frequently visited (by wall or corner, etc.)
- (2) If there are multiple landmarks in a map environment, the placement should not be too dense to cover the map environment.

In this way, a localized landmark database can be initially established, and the method of integrating visual information and laser data in Section 3.2 can be

used to obtain the location coordinates of each landmark object on the map. The details are shown in Section 3.2.

### 3.2 The Establishment of the Mapping between the Landmark Name and the Location Coordinate

In the process of mapping, the algorithm determines the available landmarks in the current environment according to the constraints of the landmark library system and creates the connection between the landmark name and the global position coordinate in the localized landmark database. The details of the process is shown in Algorithm 1.

First, the laser data is clustered by a clustering algorithm to obtain the clustered label for the laser scanning. Then, the clustered laser is fused with the object semantics to give a semantic label to each laser scanning point. The laser data with same type can be clustered into the same laser cluster. For each laser cluster, multiple laser points are included, which means there may be multiple labels and probabilities for each laser scanning point.

The semantic information of objects, such as landmarks, is obtained through visual recognition algorithms, in which the position information of each object in the environment is obtained by scanning the surrounding environment with laser radar. Based on this, the fusion of the visual detection results and the information of laser radar can be completed to generate semantic laser data. Each element in the semantic laser data contains not only the original position information of the laser scanning point, but also the object label and the corresponding probability of the label.

---

**Algorithm 1.** The creation of the connection between the landmark name and the position coordinate

---

- (a) Fusing the vision data and laser data
  - (b) Recording the global position coordinate of the object
  - (c) If the object cannot be matched in the cloud landmark database: go to (a)  
else: filtering out candidate landmarks
  - (e) Getting the location data of landmarks based on IIoT
  - (f) If the positional relationship between the candidate landmarks does not meet the constraints: go to (a)
  - (g) else: searching valid landmarks and building an effective landmark library
  - (h) Recording the semantic names and position coordinates of valid landmarks
  - (i) Creating the association mapping table
- 

The above fusion method can be used to obtain the semantic laser data, which is used to set an effective landmark, of the objects. In this way, the GMapping algorithm can be used to convert the relative local

coordinates of the object into the global coordinates of the current map. When the semantic labels and label probabilities of the objects are obtained, the label probability of each object is combined with the data content in the cloud landmark database established in Section 3.1 to compare candidate landmarks. Then, whether the landmark objects can be used in the current environment is automatically determined according to the position constraint of the candidate landmark. The information contained in the landmark  $M$  can be expressed by the following formula,

$$M = \{(x_1^g, y_1^g, K_1), (x_2^g, y_2^g, K_2), \dots, (x_m^g, y_m^g, K_m)\} \quad (1)$$

where  $g$  is the global coordinate system with the center of the world map as the origin,  $m$  is the number of valid landmarks in the current environment,  $x_m^g$  and  $y_m^g$  are the abscissa and ordinate of the  $m$ th landmark in the global Cartesian coordinate system, respectively, and  $K_m$  is the semantic name of the  $m$ th landmark.

The mapping between the landmark name and landmark global location coordinates can be created in the local landmark database according to equation (1), as shown in Table 1.

**Table 1.** The mapping between the landmark name and the location coordinate

Landmark name	indicator	Monitor Stand	Cabinet air conditioner
Global coordinates /m	(8.71, 5.53)	(14.21, 6.73)	(15.28, 9.37)

In this way, each landmark object is regarded as a point on the map in the followed position correction process, which is not affected by the robot observation location and observation angle (shown in Section 3.5).

### 3.3 Data Acquisition

#### 3.3.1 The Global Coordinates of the Landmark Object

As aforementioned, the global coordinates of the landmark objects on the map can be directly obtained by using the mapping table created based on formula (1), after the establishment of the map and the local landmark database has been completed. However, as there are multiple landmark objects in the mapping table, the machine must be filtered and searched by the landmark name to select the correct one.

Currently, the mainstream approach for visual detection is adopting deep learning algorithms for identifying the object. However, by comparing the existing object detection algorithms, we found that they cannot meet the requirements of this paper well in terms of real-time performance and accuracy. For this reason, an A-YOLOv3 (Adaptive YOLOv3) algorithm is designed in this paper based on the studying of the

YOLOv3-Tiny algorithm.

First, the training-detection model is further trained under the experiment scenario of this paper. The first step is adding the target detection datasets corresponding to the current environment with data enhancement operation on them. Based on the consideration of factors, such as distance, background environments and conditions, the real objects are sampled. Then, the tool program is used to perform random type enhancement on the sampled pictures (enhancement types include adjusting saturation, brightness, contrast, flipping left and right, rotating 0 ~ 60 degrees, etc.). The entire proof set is repeatedly enhanced 5 times to obtain a valid data set. The second step is resetting the classification method for the visual detection model according to the actual environment, and classifying the identifiable landmark. Last, the k-means function is used to calculate the initial sizes of the candidate frames of 9 types based on the data set

obtained in the first step with the target of improving the recognition accuracy, before determining the initial values of several basic parameters (learning rate, decay rate, etc.). Based on this, the effective data set can be used to continually train the model for adapting the algorithm to special environments.

In addition, a feature figure with the size of  $52 \times 52$  (corresponding candidate frames are (10, 13), (16, 30), (33, 23)) is added to increase the accuracy of the recognition of the small object with long-distance, of which the principle is that the feature figure with larger size corresponds to the candidate frame with smaller size and a smaller target to be identified, as shown in Figure 4. In Figure 4(a) and Figure 4(b) belong to the scenario that the feature figure has a small size ( $3 \times 3$ ) with a larger candidate frame, and (c) and (d) are the scenario that a feature figure has a large size of  $6 \times 6$  with a small candidate frame.

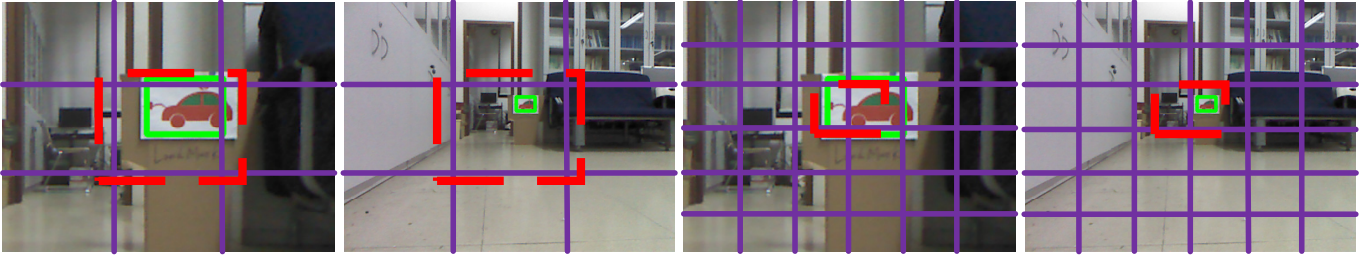


Figure 4. Schematic diagram of the candidate box selection

Though the detection speed of the new algorithm has no obvious change compared with YOLOv3-Tiny algorithm after adding the feature figure with a size of  $52 \times 52$ , the accuracy decreases. The reason is that the number of basic network layers, which are employed for extracting features, is too small and too shallow (a total of 15 layers). It means the network layers used to extract the candidate frame with a  $52 \times 52$  feature figure is too close to the input, which leads to the fine-grained extraction is not enough and the features are not fully extracted. Therefore, YOLO3-Tiny's basic network is added to the corresponding convolutional layers to enhance feature extraction.

Based on the above steps, the semantics of each object in the current operation environment can be obtained. Then, the local landmark database is searched and matched through semantic information, and the global coordinates of the landmark objects on the world map can be obtained.

### 3.3.2 The Local Coordinates of the Landmark Object

In order to ensure the accuracy of the data source, the ALA (Adaptive Location Algorithm) algorithm uses laser radar to obtain the local coordinates of the

landmark, which can avoid the deviation of the visual sensor caused by environmental factors such as light. By fixing the position relationship between the laser radar and the robot, the local coordinate system established by the laser radar can establish fixed association with the coordinate system of the robot.

Taking the rplidar-a2 laser radar as an example, the data scanning interval of the laser radar is set to 0.5 degrees (resolution), and the scanning range is set to 180 degrees, of which a total of 361 data points can be scanned. It can be seen that the angle  $\theta_j$  of each point in the polar coordinate system is:

In Figure 5, it is assumed that  $R_i$  is the  $j$ th laser point corresponding to the  $i$ th landmark near the robot. The Cartesian coordinates of the  $i$ th landmark object in the local coordinate system are:

$$x_i^l = d_j \cdot \cos \theta_j \quad (3)$$

$$y_i^l = d_j \cdot \sin \theta_j \quad (4)$$

$$\theta_j = \frac{j}{360} \cdot \pi \quad (2)$$

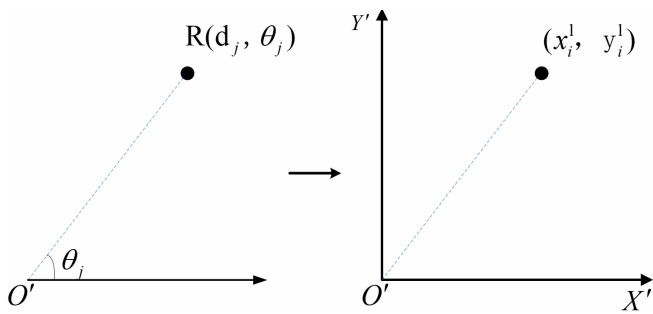


**Figure 5.** The creation of the local coordinate system by taking the robot as the origin of the coordinate system

The IMU (Inertial Measurement Unit) is a tool for recording the motion information such as acceleration and angular velocity. The gyroscope included in the IMU can records the rotational speed and heading angle of the robot motion. After calibrating, IMU can obtain the angular with high precision and high robustness. Therefore, IMU is used as a data source to obtain the deflection angle  $\alpha$  of the robot.

### 3.4 Odometer Data Source Selection

#### 3.4.1 The Q-Learning Algorithm for Positioning

In this section, reinforcement learning is adopted to optimize the point fixing during the navigation. However, it is different from the traditional path planning application. In traditional path planning applications, an  $n * n$  grid is designed and a sub-grid is selected according to the principle: choosing a path plan to the end point without traversing all the sub-lattices. In this paper, the data selection process is designed based on the principle of improving the adaptation of the algorithm. In order to apply the reinforcement learning to the selection of the odometer data source, each variable is uniqueness should be ensured, and a point which can connect both the starting point and the ending point in the original  $n * n$  grid should be confirmed. The trainings are carried out on the same path, and the running results are compared to confirm the rationality of each optimal choice. The path contains  $n$  states (target points), and only one action selection is used in the state changes. There are 4 action selections: encoder data, IMU data, laser odometer data, and vision. After completing the selection of odometer data, the robot jumps to the next state point of the path. After adapting the mechanism of the reinforcement learning, the selected sub-grid path needs be converted into Q-table in the next step. In Figure 6, each column represents the selection of four odometer data sources, while the row represents

the current state, and the value of each cell represents the corresponding state in the Q-table. The maximum future reward expectation value (Q value) is selected by the selection action, which is the basis for each subsequent action selection.

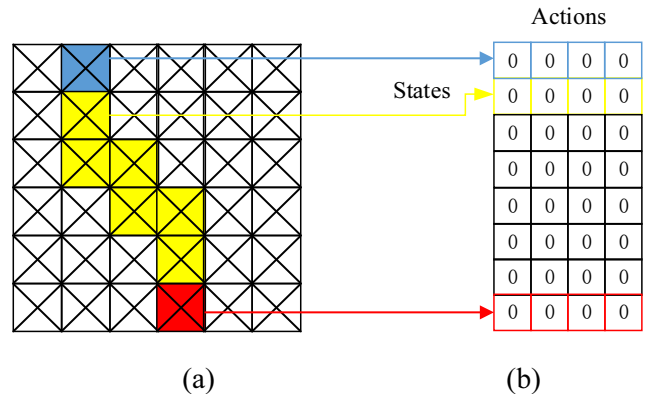


**Figure 6.** A grid map created to fit the Q-learning algorithm

For example, By dividing the current running environment into a grid of  $6 * 6$  regions and selecting a path consisting of 8 sub-grids, the grid can be converted into a  $8 * 4$  Q-type table, as shown in Figure 6, where the column, row and cell represents the four candidate odometer data sources, the states to be executed and the stored corresponding Q value, respectively.

#### 3.4.2 Optimization of the Positioning Results

First, the Q-table converted from the sub-grid path in Figure 6 is initialized, and the initial value of each cell is set to zero. At the current running state point  $s$ , the odometer data source used in the next step is selected based on the current Q value estimation. Using the learning action value function combined with the moving distance cost, the reward value  $r$  under the condition that the robot runs to the next state point and the current Q value are estimated. Combining the obtained  $r$  and Q with the Bellman equation, the Q in the Q-table is updated. Using the relocalization method, the estimated robot pose of each state point is corrected to ensure uniform operation trajectory during the training of the robot. The correction process is shown in Figure 7. Finally, the intensive training operation is repeated, and the selection action of the odometer data source is continually performed to update the reward expectation until the selection result with highest positioning accuracy in the current environment is found or the intensive training is manually stopped.

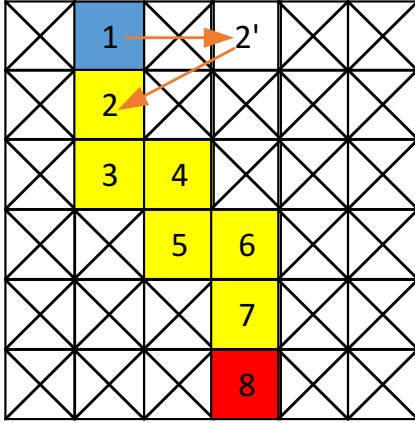


**Figure 7.** Robot positioning adjustment process

In the process of intensive training on the selection of the odometer data source, the robot will arbitrarily divide multiple trajectories in the current environment, and sequentially complete the odometer data source selection action on these trajectories to update the reward expectation. Therefore, the selection of the trajectory can be performed with a cover of the entire map environment as much as possible.

### 3.5 Pose Derivation

During the navigation process, the ALA algorithm is used to estimate the real-time location of the robot with accurate landmark information when the robot pose estimation bias occurs. Therefore, it is necessary to establish the global location  $(x_i^g, y_i^g)$  and the local location  $(x_i^l, y_i^l)$  of the landmark in the world coordinate system, and the mathematical model for the robot's real-time location conversion. Figure 8 shows the coordinate transformation method for building the relative relationship between the global coordinate system and the local coordinate system.

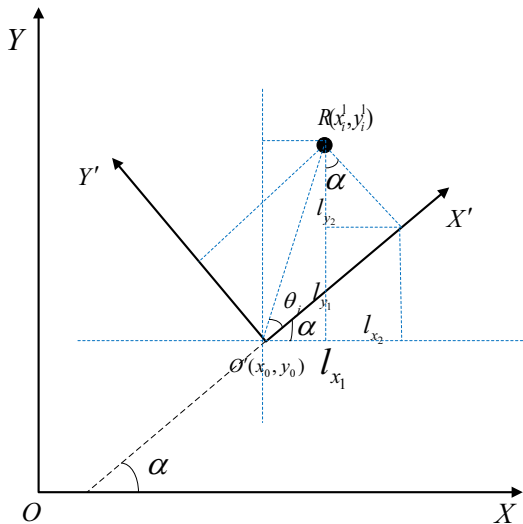


**Figure 8.** The coordinate transformation between the global coordinate system and the local coordinate system

In Figure 8,  $O$  is the origin of the world map (global coordinate system),  $O'$  is the real-time location of the robot, and a local coordinate system is constructed with it as the origin, and  $\alpha$  is the deflection angle of the robot relative to the global coordinate system. The real-time location coordinate of the robot is set to  $(x_0, y_0)$ , which can be derived through the conversion relationship:

$$x_0 = x_i^g - (l_{x_1} - l_{x_2}) \quad (5)$$

$$y_0 = y_i^g - (l_{y_1} + l_{y_2}) \quad (6)$$

where  $l_{x_1}$ ,  $l_{x_2}$ ,  $l_{y_1}$ ,  $l_{y_2}$  can be derived from the local coordinates and angles of the landmark  $R$ . Figure 8 only shows the coordinate conversion relationship of the first quadrant. Due to the diversity of actual conditions, landmark objects may also be in other quadrants of the robot's local coordinate system. The deduction of the actual position of the robot can be summarized as:

$$\begin{pmatrix} x_0 \\ y_0 \end{pmatrix} = \begin{pmatrix} x_i^g \\ y_i^g \end{pmatrix} - \begin{pmatrix} \cos \alpha & -\sin \alpha \\ \sin \alpha & \cos \alpha \end{pmatrix} \begin{pmatrix} x_i^l \\ y_i^l \end{pmatrix} \quad (7)$$

According to the algorithm proposed in this paper, the real-time location coordinate  $(x_0, y_0)$  of the robot and its heading angle  $\alpha$  can be quickly and accurately calculated according to the multi-class sensor data and landmark object information. The relocalization process is shown in Figure 9.



**Figure 9.** The process of correcting the pose by using the landmark

In summary, the algorithm only needs to input visual information and laser data, and can complete pose derivation by means of landmark objects.

## 4 Evaluation

### 4.1 Experiment Platform

In order to verify the effectiveness and innovation of the ALA, the intelligent platform shown in Figure 10 is built. It consists of PC, camera, laser radar, IMU and mobile base. The data transmission is carried out under the ROS mechanism, in which the main algorithm is run by the PC.

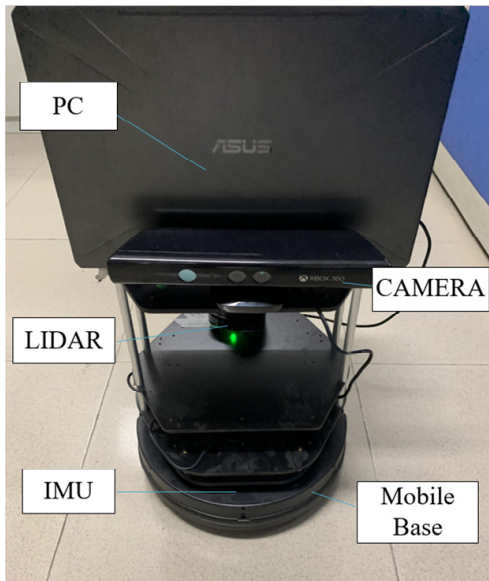


Figure 10. The experiment platform

The specific hardware configuration of the platform is: a monocular vision sensor with a resolution of 640×480, i7-8750H PC CPU, GeForce GTX 1060 graphics card, Kobuki mobile base, a L3G4200D model 3-axis digital gyroscope for the IMU and a laser sensor with a rate of up to 0.5mm.

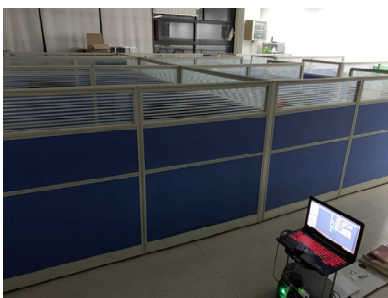
The experiment environment in this paper is an actual scene of about 60 square meters. The grid map initially constructed based on the laser radar is shown in Figure 11. In order to verify the superiority of the proposed ALA algorithm in intelligence and accuracy, a complicated scene with a lot of obstacles and similar parts is set in the experiment environment.

The whole experiment environment can be divided into three parts, as shown in Figure 12, where Figure 12(a) corresponds to the part A in Figure 11, which has fewer obstacles, but many similar environments with low light intensity. Figure 12(b) corresponds to the part B of Figure 11, where there are fewer obstacles with higher light intensity. Figure 12(c) corresponds to the part C of Figure 11, where the environment is much complicated, in which the movable space is small with a lot of obstacles.

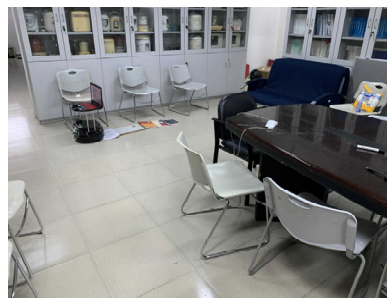
Since some odometer data sources are susceptible to the pitch angle of the robot during navigation, the stepped road surface in Figure 13 is specially set to verify the anti-jamming effect of the algorithm.



Figure 11. The raster map of the experiment environment



(a) Part A



(b) Part B



(c) Part C

Figure 12. Experiment environment



Figure 13. Simulation on the uneven ground

## 4.2 The Relocalization Algorithm

Due to the cumulative error generated by the range derivation algorithm, the pose of the robot during the navigation process will gradually drift. Therefore, in order to ensure that the adaptive positioning algorithm of this paper is not affected by the accumulated error during the navigation process, it is necessary to determine the pose offset of the next state without the

interference of the previous state when the robot positioning is intensively trained. Relocalization is required to eliminate the accumulated error.

### 4.2.1 Relocalization Results

In the intensive training process of the ALA algorithm, the  $i-1$ th state point is navigated to the  $i$ th state point. At this time, the pose deviation may have been generated. In addition, the offset will be passed to the  $i$ th state point if it is not eliminated. With navigating to the next state point, the factors caused by the positional deviation at the state point cannot be determined according to the error, which means that the credibility of the experimental results of the algorithm cannot be guaranteed. Therefore, in order to ensure that the positioning deviation of the  $i+1$ th state point is not interfered by the error caused by the previous state, it is necessary to use the relocalization algorithm to correct the current pose deviation before navigating to the next state point. Figure 14 shows the relocalization process at a certain state point during navigation.

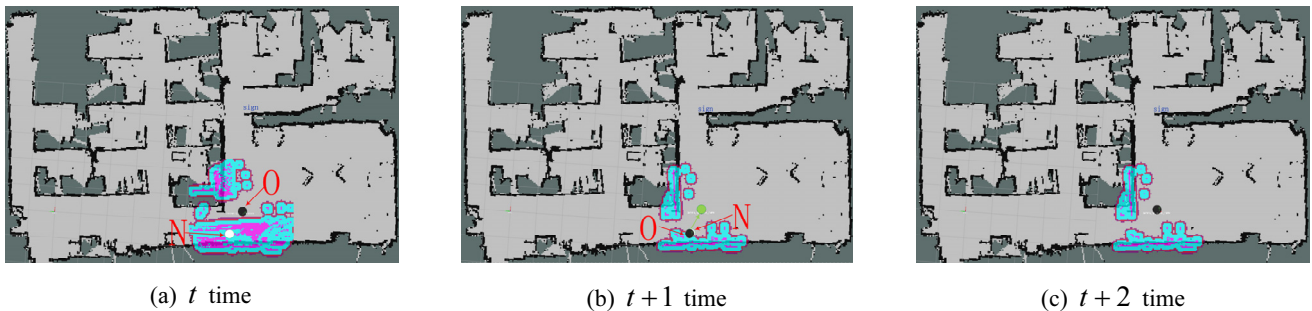


Figure 14. The relocalization result at a certain state point

The relocalization algorithm in this paper reverses the actual position of the robot by using landmark object. The position correction effect of the algorithm can be seen from the experiment process in Figure 14. The part enclosed by black and gray is the map representation of the current environment. The white circle  $N$  in Figure 14(a) is the actual position of the robot at time  $t$ , and the black circle  $O$  is the position misjudged in the map. As the pose deviation has already occurred at this time, the robot cannot directly navigate from the position of the white circle  $N$  to the next state point, which means the position of the black circle  $O$  needs to be corrected by the landmark at  $t+1$  time. After the position is corrected, the robot continues to move to the current state point (green circle position) until the relocalization is completed at time  $t+2$  so that the navigation process of the next state can be entered, which can be seen that the algorithm has a high relocalization performance.

### 4.2.2 Visual Recognition Results

The relocalization process is carried out under the assistance of the landmark information, in which the corresponding semantic information and local coordinates are obtained by visually recognizing the landmark objects in the surrounding environment. Therefore, the AIR (Adaptive Intelligent Recognition) algorithm proposed in this paper should be experimentally verified. The verification under the near and far distance (4.0m and 1.5m) is carried out in three parts of the whole experiment environment. The recognition results are shown in Figure 15 and Figure 16.

Figure 15(a) is the recognition result of the landmark object in the environment which is relatively simple but the overall illumination intensity is low. Figure 15(b) is the recognition result of the landmark object in B part of the experiment environment where the environment is brighter and the obstacles are less. Part

(c) is the recognition result of the landmark object in the experiment environment which the environment is relatively complicated with many obstacles. The identification result is framed and be given a semantic tag.

Figure 16 is the result of the landmark object from a long distance, in which part (a) is the recognition result of the landmark object in the part A of the experimental environment. Part (b) is the recognition result of the landmark object in the part B of the experimental environment, and Part (c) is the result

corresponding to the part C of the experimental environment.

Compared to other recognition algorithms in the current experiment scene, we see that the proposed AIR algorithm cannot achieve the best detection speed and accuracy at the same time. However, it can greatly improve the recognition accuracy when only adding some response time. To meet the daily navigation needs, the performance comparison is shown in Figure 17.

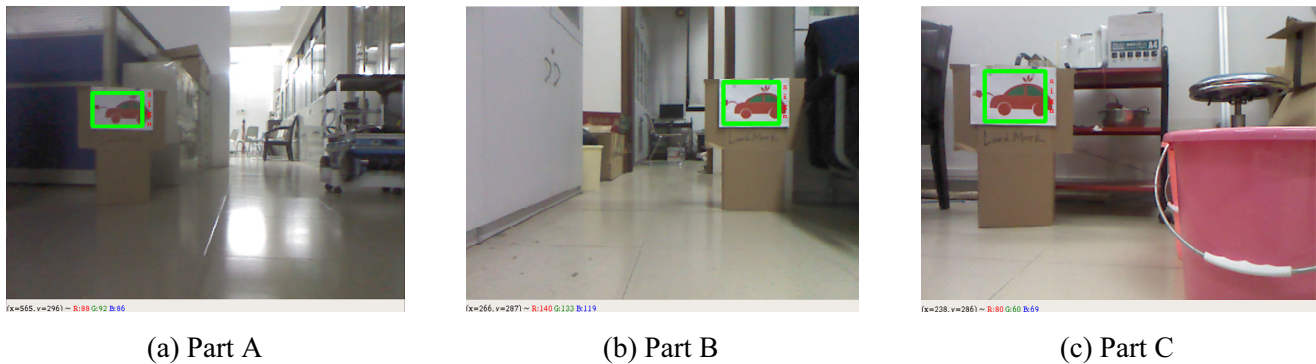


Figure 15. The results of the short-distance visual recognition

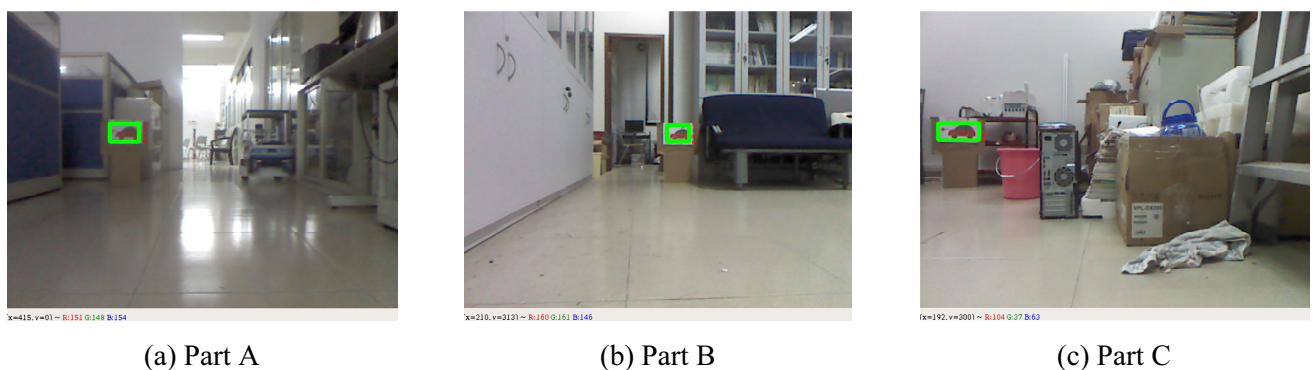


Figure 16. The results of the long-distance visual recognition

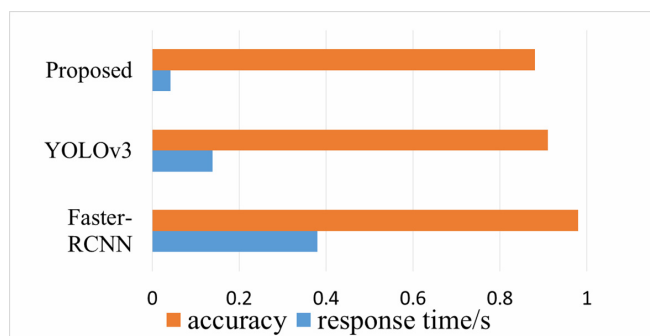


Figure 17. Performance comparison between different recognition algorithms

### 4.3 The adaptive Positioning Algorithm

It has been verified in Section 4.2.1 that the relocalization algorithm can achieve high pose-correction performance and eliminate certain pose

deviations. However, it can only be regarded as the back-end optimization method, in which the landmark is passed after each determination of the robot positioning. It cannot solve the problem fundamentally that the object reversely corrects its own pose deviation. The ALA (Adaptive Positioning) in this paper is designed to strengthen the training when the robot selects its odometer data source to ensure that the optimal amount of motion information can be obtained at each state point to enable the robot to complete the positioning. This part is the designed experiment to verify the actual effect of the proposed ALA algorithm.

#### 4.3.1 Experiment Design

In order to verify the robustness and effectiveness of the proposed ALA algorithm, the robot repeatedly navigates 60 times across the path which is divided into 43 grid regions, as shown in Figure 20, in which

the robot is allowed to continually perform intensive training between each state point to dynamically filter the odometer data source. During the whole experiment, we observe the deviation between the actual position trajectory of the robot and the set trajectory.

The orange line in Figure 18 encloses the navigation route set by the current experiment. The route spans the three parts in Figure 11 in the experimental environment to ensure the effectiveness of the experiment data. This section normalizes the navigation path and records the pose state of each grid in order to observe the experiment results more clearly. When the robot (black circle) navigates from one state point to the next, it will intensively train the selection of the odometer data source.

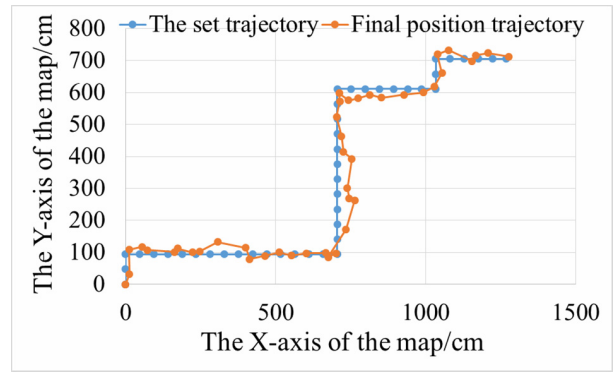


Figure 18. The navigation path

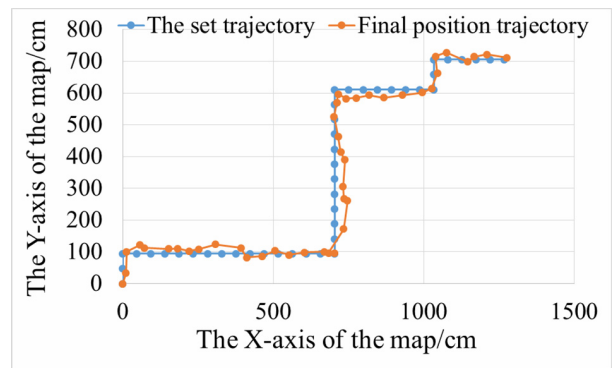
### 4.3.2 The Intensive Training Performance

According to the above experiment scheme, the robot uses the ALA algorithm to perform autonomous navigation on the specified route. The actual position coordinates are recorded when the robot navigates to each state point (the global coordinate system of the map established with the initial point of the robot positioning as the origin, see Figure 18). The final position trajectory is compared with the set trajectory, and the posture deviation is observed, as shown in Figure 19.

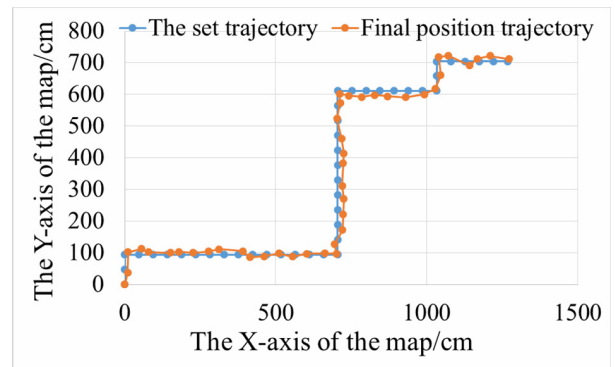
In Figure 19, the navigation process is repeated sixty times on the designed route, and the selection result of the training odometer data source is continuously enhanced. The blue route is the set trajectory of each state point, which is also the ideal navigation trajectory of the robot. The orange route is the actual position trajectory recorded during the navigation process. Analyzing the experiment data in Fig. 19, we can see that the actual pose trajectory is getting closer and closer to the set state point trajectory as the robot repeats the navigation process.



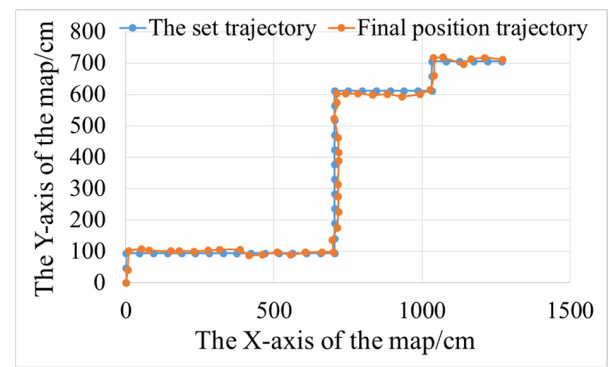
(a) First pose trajectory



(b) The 10th pose trajectory



(c) The 30th pose trajectory



(d) The 60th pose trajectory

Figure 19. Robot pose results

### 4.3.3 The Performance of the Traversing

The above experiments show that the data source of the enhanced odometer data will be more and more reliable and the positioning accuracy will be higher and higher as the number of navigations on the designed route increases. Therefore, the positioning performance in the whole experiment scene can be improved by performing navigation training in various parts of the map environment, as shown in Figure 20. The green, orange and red lines represent each robot travel path, respectively, which can be effectively traversed by the selection method.



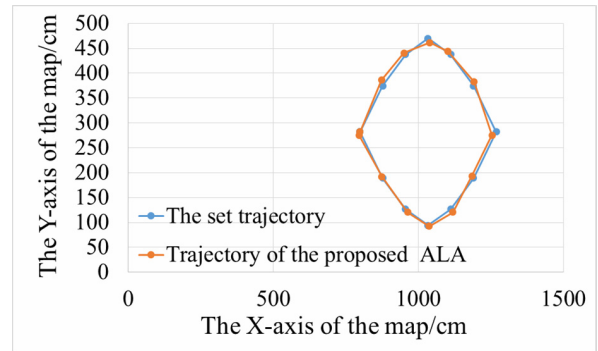
Figure 20. Paths for traversing the overall environment

## 4.4 The Comparison on the Positioning Performance

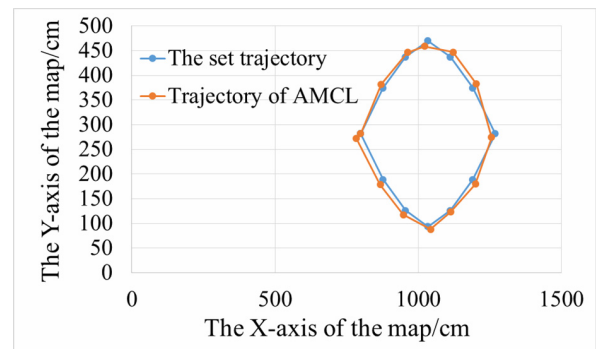
Since the global coordinates of the landmarks used in the algorithm are obtained by visually recognizing the landmarks and finding the matching association mapping table, the A-YOLOv3 algorithm is proposed in this paper to adapt the real-time and accuracy requirements from relocalization algorithms. In order to verify the feasibility of the A-YOLOv3 recognition algorithm, the experiment results are verified under the conditions of short distance and long distance (1.5m and 3.5m) with bright (more than 300 lux) and dark visual environment (less than 200 lux), respectively.

### 4.4.1 The Comparison on Pose Trajectory

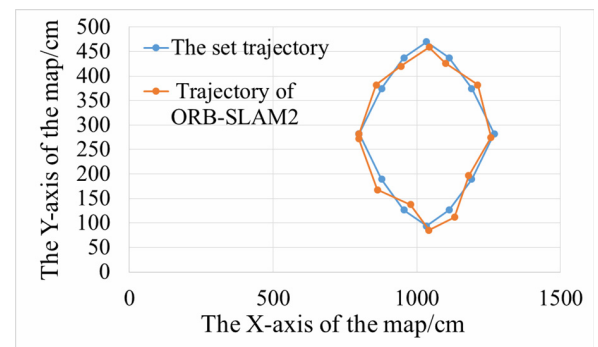
The robot navigates on a closed loop route with fourteen state points. Figure 21(a), Figure 21(b) and Figure 21(c) show the pose of the proposed ALA algorithm, AMCL algorithm and ORB-SLAM2 algorithm, respectively. The blue-color line indicates the set trajectory for the state points, which is also the ideal navigation trajectory of the robot, and the orange route is the recorded actual position trajectory.



(a) The proposed algorithm



(b) AMCL algorithm



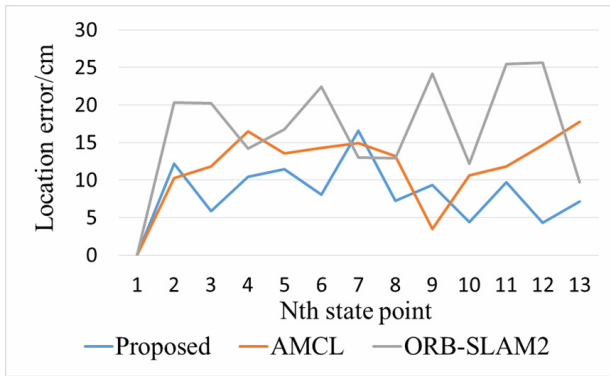
(c) ORB-SLAM2 algorithm

Figure 21. The pose trajectory on closed loop route

It can be seen from Figure 21 that the actual pose trajectory recorded by the ALA algorithm is closest to the set trajectory and can return to the initial point at the last moment to form a closed loop in the loopback route.

### 4.4.2 The Comparison on Pose Deviation

In order to better reflect the positioning performance of the proposed ALA algorithm, the Euclidean distance formula  $d = \sqrt{(x - x')^2 + (y - y')^2}$  is used to calculate the error between the actual position and the set position (state point position) of the robot on the current loopback line. The comparison of the positioning error during the whole operation is shown in Figure 22.



**Figure 22.** Positioning error of each algorithm during operation

To show the quantified accuracy and the stability of the algorithm, the mean value and variance of the positioning error is also evaluated, as shown in Table 2.

**Table 2.** The mean and variance of the positioning error

	AMCL	ORB-SLAM	ALA
mean error /cm	About 11.8	About 16.7	About 8.2
error variance /cm	About 12.3	About 29.1	About 11.4

## 5 Conclusion

The relocalization algorithm in this paper is proposed based on optimizing the positioning of the current mainstream SLAM algorithm. An ALA algorithm employing visual sensor to simulate the human eye is designed, which is used to identify the objects and landmarks around the robot. The laser and IMU are used to obtain information with high accuracy. Based on the assistance of IIoT, an effective landmark database system is designed. A pose derivation model based on the acquired landmark information is presented to correct the position of the actuator. In addition, the reinforcement learning is employed to dynamically select the optimal motion information during the relocalization process. The experiment results show the relocalization algorithm designed in this paper has good performance in accuracy and stability, in which the total localization deviation is about 8.2cm and the variance is about 11.4cm.

## Acknowledgments

This work was supported in part by grants from the National Natural Science Foundations of China (No.61701122), the Natural Science Foundation of Guangdong Province, China (Nos. 2019A1515011056, 2018A030310540, 2018A030313868), Science and Technology Program of Guangzhou, China (No. 201804010238).

## References

- [1] M. Aazam, S. Zeadally, K. Harras, Deploying Fog Computing in Industrial Internet of Things and Industry 4.0, *IEEE Transactions on Industrial Informatics*, Vol. 14, No. 10, pp. 4674-4682, October, 2018.
- [2] M. Aazam, K. Harras, S. Zeadally, Fog Computing for 5G Tactile Industrial Internet of Things: QoE-Aware Resource Allocation Model, *IEEE Transactions on Industrial Informatics*, Vol. 15, No. 5, pp. 3085-3092, May, 2019.
- [3] J. Wan, B. Chen, M. Imran, F. Tao, D. Li, C. Liu, S. Ahmad, Toward Dynamic Resources Management for IoT-based Manufacturing, *IEEE Communications Magazine*, Vol. 56, No. 2, pp. 52-59, February, 2018.
- [4] D. Miao, L. Liu, R. Xu, J. Panneerselvam, Y. Wu, W. Xu, An Efficient Indexing Model for the Fog Layer of Industrial Internet of Things, *IEEE Transactions on Industrial Informatics*, Vol. 14, No. 10, pp. 4487-4496, October, 2018.
- [5] M. Al-Hawawreh, F. Hartog, E. Sitnikova, Targeted Ransomware: A New Cyber Threat to Edge System of Brownfield Industrial Internet of Things, *IEEE Internet of Things Journal*, Vol. 6, No. 4, pp. 7137-7151, August, 2019.
- [6] J. Wan, S. Tang, Z. Shu, D. Li, S. Wang, M. Imran, A. Vasilakos, Software-Defined Industrial Internet of Things in the Context of Industry 4.0, *IEEE Sensors Journal*, Vol. 16, No. 20, pp. 7373-7380, October, 2016.
- [7] K. Choo, S. Gritzalis, J. Park, Cryptographic Solutions for Industrial Internet-of-Things: Research Challenges and Opportunities, *IEEE Transactions on Industrial Informatics*, Vol. 14, No. 8, pp. 3567-3569, August, 2018.
- [8] X. Li, D. Li, J. Wan, C. Liu, M. Imran, Adaptive Transmission Optimization in SDN-Based Industrial Internet of Things with Edge Computing, *IEEE Internet of Things Journal*, Vol. 5, No. 3, pp. 1351-1360, June, 2018.
- [9] J. Liu, J. Wan, D. Jia, B. Zeng, D. Li, C. Hsu, H. Chen, High-efficiency Urban traffic Management in Context-aware Computing and 5G Communication, *IEEE Communications Magazine*, Vol. 55, No. 1, pp. 34-40, January, 2017.
- [10] F. Aini, A. Jati, U. Sunarya, A study of Monte Carlo Localization on Robot Operating System, *2016 International Conference on Information Technology Systems and Innovation*, Bandung, Indonesia, 2016, pp. 1-6.
- [11] R. Guan, B. Ristic, L. Wang, Combining KLD-sampling with Gmapping Proposal for Grid-based Monte Carlo Localization of a Moving Robot, *20th International Conference on Information Fusion (Fusion)*, Xi'an, China, 2017, pp. 1-8.
- [12] T. Chau, W. Luk, P. Cheung, A. Eele, J. Maciejowski, Adaptive Sequential Monte Carlo Approach for Real-time Applications, *22nd International Conference on Field Programmable Logic and Applications (FPL)*, Oslo, Norway, 2012, pp. 527-530.
- [13] M. Qomaruddin, A. Alasiry, N. Tamami, Routing Algorithm in Legged Robot with Dynamic Programming and Monte Carlo Localization, *2017 International Electronics Symposium on Engineering Technology and Applications (IES-ETA)*, Surabaya, Indonesia, 2017, pp. 281-286.

- [14] M. Hasan, M. Abdellatif, Experimental Verification of Direct Depth Computing Technique for Monocular Visual SLAM Systems, *First International Conference on Innovative Engineering Systems*, Alexandria, Egypt, 2012, pp. 142-147.
- [15] A. Kasyanov, F. Engelmann, J. Stückler, B. Leibe, Keyframe-based Visual-inertial Online SLAM with Relocalization, *2017 IEEE/RSJ International Conference on Intelligent Robots and Systems (IROS)*, Vancouver, Canada, 2017, pp. 6662-6669.
- [16] N. Ragot, R. Khemmar, A. Pokala, R. Rossi, J. Ertaud, Benchmark of Visual SLAM Algorithms: ORB-SLAM2 vs RTAB-Map, *2019 Eighth International Conference on Emerging Security Technologies (EST)*, Colchester, United Kingdom, 2019, pp. 1-6.
- [17] A. Yoon, J. Kwon, F. Park, A Loop Closure Technique for Monocular SLAM with Locally Planar Landmarks, *10th International Conference on Ubiquitous Robots and Ambient Intelligence (URAI)*, Jeju, South Korea, 2013, pp. 602-603.
- [18] R. Mur-Artal, J. Tardós, ORB-SLAM2: An Open-source Slam System for Monocular, Stereo, and RGB-D Cameras, *IEEE Transactions on Robotics*, Vol. 33, No. 5, pp. 1255-1262, October, 2017.
- [19] S. Fujimoto, Z. Hu, R. Chapuis, R. Aufrère, ORB-SLAM Map Initialization Improvement Using Depth, *2016 IEEE International Conference on Image Processing (ICIP)*, Phoenix, AZ, USA, 2016, pp. 261-265.
- [20] Y. Endo, K. Sato, A. Yamashita, K. Matsubayashi, Indoor Positioning and Obstacle Detection for Visually Impaired Navigation System Based on LSD-SLAM, *2017 International Conference on Biometrics and Kansei Engineering (ICBAKE)*, Kyoto, Japan, 2017, pp. 158-162.
- [21] L. Zhenjun, H. Nisar, A. Malik, A Framework for Real Time Indoor Robot Navigation using Monte Carlo Localization and ORB Feature Detection, *The 18th IEEE International Symposium on Consumer Electronics (ISCE)*, JeJu Island, South Korea, 2014, pp. 1-2.
- [22] H. Wei, X. Li, Y. Shi, B. You, Y. Xu, Multi-sensor Fusion Glass Detection for Robot Navigation and Mapping, *2018 WRC Symposium on Advanced Robotics and Automation (WRC SARA)*, Beijing, China, 2018, pp. 184-188.
- [23] K. Lekkala, V. Mittal, Accurate and Augmented Navigation for Quadcopter Based on Multi-sensor Fusion, *2016 IEEE Annual India Conference (INDICON)*, Bangalore, India, 2016, pp. 1-6.
- [24] T. Tongloy, S. Chuwongin, K. Jaksukam, C. Chousangsuntorn, S. Boonsang, Asynchronous Deep Reinforcement Learning for the Mobile Robot Navigation with Supervised Auxiliary Tasks, *2nd International Conference on Robotics and Automation Engineering (ICRAE)*, Shanghai, China, 2017, pp. 68-72.
- [25] R. Kamoshida, Y. Kazama, Acquisition of Automated Guided Vehicle Route Planning Policy Using Deep Reinforcement Learning, *6th IEEE International Conference on Advanced Logistics and Transport (ICALT)*, Bali, Indonesia, 2017, pp. 1-6.
- [26] A. Pambudi, T. Agustinah, R. Effendi, Reinforcement Point and Fuzzy Input Design of Fuzzy Q-Learning for Mobile Robot Navigation System, *2019 International Conference of*

*Artificial Intelligence and Information Technology (ICAIT)*, Yogyakarta, Indonesia, 2019, pp. 186-191.

- [27] R. Li, L. Fu, L. Wang, X. Hu, Improved Q-learning Based Route Planning Method for UAVs in Unknown Environment, *IEEE 15th International Conference on Control and Automation (ICCA)*, Edinburgh, United Kingdom, 2019, pp. 118-123.

## Biographies



**Bi Zeng** received the M.S. and Ph.D. degrees from Guangdong University of Technology (GDUT). She is currently a Professor with the School of Computers, GDUT. Her current research interests include computational intelligence, data mining, intelligent robot, and wireless sensor networks.



**Shuang Yang** received his B.E. degree in Software Engineering from Nanchang Hangkong University, China in 2017. He is currently pursuing the Master's degree in Computer Science from Guangdong University of Technology. His current research interests include intelligent robot and computational intelligence.



**Xiuwen Yin** received his Ph.D. degree in communication and information system from Sun Yat-sen University, China, in 2015. He is currently a lecturer with the School of Automation, Guangdong University of Technology, China. His current research interests include wireless communication, Internet of vehicle, Internet of things and signal processing.